DESIGN AND EXPERIMENT OF NO-TILLAGE PLANTER FOR HIGH AND LOW BORDERS WHEAT
/
高低畦小麦免耕播种机设计与试验

Shandong YANG[1], Chuang MA[1], Baochang Zhang*[1], Yinping ZHANG[1], Jinchang YANG[2]

[1]School of Agricultural and Food Science, Shandong University of Technology, Zibo (255000), China;
[2]Shandong Qingyun Yiyuan Agricultural Machinery Manufacturing Co., Ltd, Zibo (255000), China;
DOI: https://doi.org/10.35633/inmateh-71-36

Keywords: *Wheat seeder, High and low borders, simulation research, ship-type ridging device*

ABSTRACT
Aiming at the problems of low land utilization and serious water waste in the existing wheat planting pattern, a two-high and two-low wheat high-low border spaced apart planting mode was proposed, and a high and low borders wheat no-till planter that can finish stubbing, fertilization, border construction, seeding and other tasks was designed. The design and analysis of the ship-type ridging device were carried out, and the construction process was simulated to determine the optimal parameters. A field test was carried out, the average sowing depth was 3.17 cm, the qualification rate was 95%, the standard deviation was 0.38 cm, and the coefficient of variation was 12.06%. The average value of the width of the seedling belt was 9.40 cm, the qualification rate was 91.67%, the standard deviation was 0.29 cm, and the coefficient of variation was 3.09%. The average height difference between the high and low borders was 9.26 cm, the pass rate was 100%, the standard deviation was 0.35 cm, and the coefficient of variation was 3.83%. The average width of the borders was 52.18 cm, the qualified rate of the border width was 100%, the standard deviation was 1.00 cm, and the coefficient of variation was 1.93%. The differences between each index and the theoretical design are small and meet the agronomic requirements.

摘要
针对现有小麦种植模式土地利用率低、水资源浪费严重的问题，本文提出了一种两高畦两低畦间隔分布的小麦高低畦种植模式，并设计了一种可一次性完成灭茬、施肥、构畦、播种等工作的高低畦小麦免耕播种机。对船式构畦器进行了设计和分析，并对构畦过程进行了仿真，确定了最优参数。田间试验表明，播种深度的平均值为 3.17cm，合格率为 95%，标准差为 0.38cm，变异系数为 12.06%；苗带宽度的平均值为 9.40cm，合格率为 91.67%，标准差为 0.29cm，变异系数为 3.09%；高低畦的高度差平均值为 9.26cm，合格率 100%，标准差为 0.35cm，变异系数为 3.83%；畦面宽度平均值为 52.18cm，合格率是 100%，标准差是 1.00cm，变异系数是 1.93%，各项指标与理论设计差异较小且符合农艺要求。

INTRODUCTION
Wheat is one of the major grain crops in China, accounting for about 20% of the current total grain crop production in China *(Yang, 2008; Li, 2006)*. With the deepening of the structural reform of the agricultural supply side, as well as the promotion of the implementation of the seasonal fallow system in some areas, the sowing area of wheat has been reduced. This has led to a reduction in the total area of planted wheat in China, and the increase in yields showed a downward trend *(Qi, 2020; Gao, 2020)*. As to how to improve wheat yield, academician Songlie Yu proposed the technology of wide precision sowing of wheat. He believes that when the width of the seedling strip is within the range of 80~100 mm, wheat can fully utilize photosynthesis, which increases yield *(Yu, 1980)*. The planting pattern of the wheat-wide seedling belt on a high-low border is distributed between high and low borders *(Song et al., 2021)*. As shown in Fig. 1, two rows of wheat are planted in the raised borders and two rows in the low borders, and when the water is irrigated in the low ridge, the high ridge will have ensured the water required for germination due to water infiltration. This model can be used in rotation with corn, planted on the sloped side of the high borders, which also saves water. Compared with the traditional border planting mode, this planting mode can effectively save water and improve wheat acre yield. Therefore, this paper designs a no-tillage wheat seeder for the high-low border, which can simultaneously complete the stubbing, fertilization, border construction, seeding, suppression, and other tasks, realizing the combination of agronomy and agro-machinery.

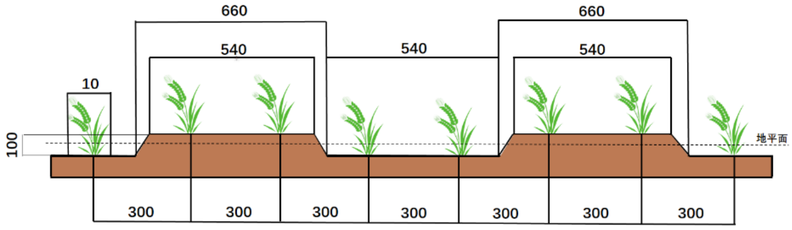

Fig. 1 - High and low borders planting mode

MATERIALS AND METHODS

The structure and working principle

The overall structure of a high-low border wheat no-till planter is shown in Fig. 2, which is mainly composed of a frame, rotary stubble device, fertilizer device, ridging device, profiling seeding device, and transmission part, and the main technical parameters of the whole machine are shown in Table 1.

The high-low border wheat no-till planter is connected to the tractor through a three-point suspension. Part of the fertilizer discharged from the fertilizer dispenser is spread to the ground through the fertilizer board. The power output shaft at the rear of the tractor connects with the main transmission through the universal joints to transfer the power to the rotating stubble device, and the stubble cutter shaft rotates at a high speed to mix the fertilizer with the soil. Driven by the tractor, the fertilizer device under the drive of the tractor, the fertilizer device, and the border construction device enter the soil in turn. The fertilizer device discharges the fertilizer into the fertilizer furrow through the chisel furrow opener to realize the function of deep fertilization. The border construction device extrudes and spreads the treated soil to both sides to form the border between high and low. The imitation sowing device imitates the shape according to the formation of the high and low borders. The seed dispenser discharges the wheat seeds into the underground seeding furrow to complete the seed dispensing operation through the double-disk wide seedling belt opener under the drive of the pressure wheel. The pressure wheel is installed at the back of the imitation sowing device and floats with the sowing unit to realize the suppression of wheat seeds.

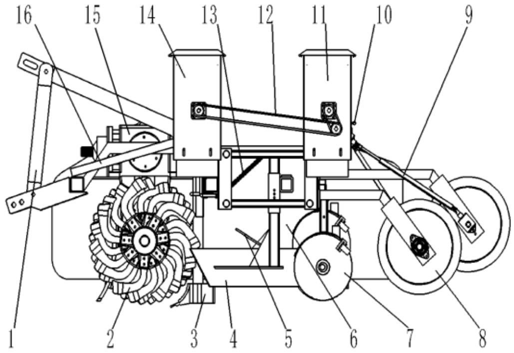

Fig. 2 - Structure diagram of the no-tillage planter for high and low borders wheat

1. Frame; 2. Rotary stubble device; 3. Fertilizer device; 4. Border framer;
5. Soil scraper; 6. Side plate; 7. Double disk wide seedling belt opener; 8. Pressure wheel;
9. Shaft drive; 10. Sowing volume adjustment gearbox; 11. Seed box; 12. Chain drive;
13. Tension spring; 14. Fertilizer box; 15. Main gearbox; 16. Fertilizer spreading plate.

Table 1

Technical parameters of the no-tillage planter for high and low-border wheat

Items	Parameters
Hook mode	Trifilar suspension
Working width /cm	240
Seeding rows	8
Seeding row spacing /cm	30
Planting depth /cm	2~4
Belt width /cm	10
Fertilization method	Deep fertilize and spread fertilizer

Critical Component Design

Design of ridging devices

(1) ***Structural design of ridging device***

In this paper, a ship-type ridging device is designed, which mainly consists of a soil divider, a fascia plate, and a connecting handle. During operation, the stubble device first treats the plot, cuts off the stubble, and throws the soil from the low-border position to the high-border centrally. Then the ship-type ridging device trellis builder squeezes and throws the soil particles so that the soil in the low-border can be fully transferred to the high-border position. It solidifies the high border surface, reduces the natural slide of soil particles, and lays the foundation for subsequent sowing process.

The upper front end of the ship-type ridging device is tilted forward to allow for easy access over the straw residue in the field, preventing it from collecting in the front of the implement and causing congestion. The sides of the ridging device are gradually tilted outward from low to high, squeezing the passing soil to both sides, creating a sloping surface for the high and low borders, and squeezing and spreading the soil particles from the low borders to the high borders *(Gou et al., 2012; Liu et al., 2021)*. According to the agronomic requirements, the width of the low border is 540 mm, and the height of the border is 100 mm. Because of the consideration of the return of soil at the end of the construction process and the compaction of the compaction wheels, the value range of the soil dividing angle α is 55~65°, the value range of the front inclination angle β is 55~65°, the width of the bottom of the ridging device is 550 mm, and the height of the ridging device is 200 mm in the vertical direction. The spatial coordinate system shown in Fig. 3(a) was established to analyse the structural parameters of the ridging device, and the forward direction of the ridging device was taken as the positive direction of the x-axis.

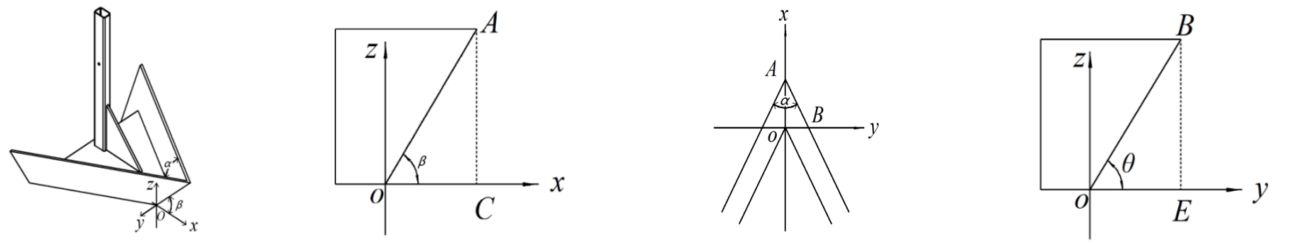

(a) space coordinates system (b) *xOz* plane geometry analysis (c) *xOy* plane geometry analysis (d) *zOy* plane geometry analysis

Fig. 3 - Geometry analysis of ridging device

The process of border construction can be regarded as an inclined plane acting on the soil, the soil particles to the two sides of the process of extrusion, selected any point on the side plate of the soil particles of the mass point o as the object of study *(Liu et al., 2017; Liu et al., 2019)*, the establishment of the mechanics of the spatial coordinate system as shown in Fig. 4, is still the direction of the forward direction of the ridging device for the x-axis positive direction, the forward speed of, the ridging device on the side of the soil particles of the instantaneous pressure for F. The process of border construction can be regarded as an inclined plane acting on the soil, the process of extrusion to the two sides of the soil particles.

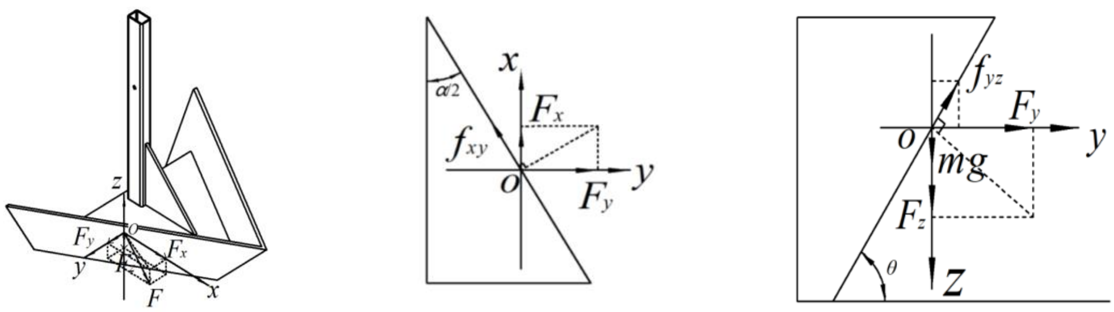

(a) Spatial stress analysis (b) *xOy* Plane stress analysis (c) yOz Plane mechanical analysis

Fig. 4 - Mechanics analysis of point squeezing of soil particles

Kinetic equations for the soil particle plasmas along the x, y, and z axes are:

$$\begin{cases} F_x + f_{xy}\cos\dfrac{\alpha}{2} = ma_x \\ F_y + f_{yz}\cos\theta - f_{xy}\sin\dfrac{\alpha}{2} = ma_y \\ F_z - f_{yz}\sin\theta + mg = ma_z \\ f_{xy} = \tan\varphi\sqrt{F_x^2 + F_y^2} \\ f_{yz} = \tan\varphi\sqrt{F_y^2 + F_z^2} \\ F_x = F_y\tan\dfrac{\alpha}{2} \\ F_z = F_y\cot\theta \\ F = \sqrt{F_x^2 + F_y^2 + F_z^2} \end{cases} \tag{1}$$

where: m - soil particle quality, (kg);

g - gravity acceleration, (N/kg);

F_x - the texture of the soil grain is subjected to the component force of the instantaneous pressure in the X-axis direction at the O point, (N);

F_y - the texture of the soil grain is subjected to the component force of the instantaneous pressure in the Y-axis direction at the O point, (N);

f_{xy} - the friction force on a particle in the *xOy* plane, (N);

f_{yz} - the friction force on a particle in the *zOy* plane, (N);

φ - soil friction angle, (°);

a_x - acceleration of a particle in the X-axis direction, (m/s^2);

a_y - acceleration of a particle in the Y-axis direction, (m/s^2);

a_z - acceleration of a particle in the Z-axis direction, (m/s^2);

It is obtained from formula (1)

$$\begin{cases} a_x = \dfrac{F\left(\tan\dfrac{\alpha}{2} + \tan\varphi\right)}{m\sqrt{1+\tan^2\dfrac{\alpha}{2}\left(\dfrac{1+\tan^2\beta}{\tan^2\beta}\right)}} \\ a_y = \dfrac{F\left[1+\tan\varphi\tan\dfrac{\alpha}{2}\left(\dfrac{1-\tan\beta}{\tan\beta}\right)\right]}{m\sqrt{1+\tan^2\dfrac{\alpha}{2}\left(\dfrac{1+\tan^2\beta}{\tan^2\beta}\right)}} \\ a_z = \dfrac{F\left(\dfrac{\tan\dfrac{\alpha}{2}}{\tan\beta} - \tan\varphi\right)}{m\sqrt{1+\tan^2\dfrac{\alpha}{2}\left(\dfrac{1+\tan^2\beta}{\tan^2\beta}\right)}} \end{cases} \tag{2}$$

From equation (2), it can be seen that the force on the soil particle mass point is related to the soil parting angle α, the front inclination angle β, and the soil friction angle φ. By Newton's third law, the force is mutual, so it can be seen that the forward resistance of the bordering device is also related to the soil parting angle α, the front inclination angle β, and the soil friction angle φ. In addition, according to the rational formula of the traction resistance of the plough, it is known that the forward speed v of the bedding device is also one of the factors affecting the forward resistance of the bedding device:

$$R = R_1 + R_2 + R_3 = fG + kab + \varepsilon abv^2 \tag{3}$$

where: R - drag resistance of plough, (N);

f - combined friction coefficient, f=0.3~0.5;

k - coefficient of resistance to deformation of soil, (N/cm^2);

a - tilling depth, (cm);

b - working width, (cm);

ε - dynamic drag coefficient, (Ns^2/m^4);

v - the forward speed of the plough, (m/s^2);

(2) *Design of structural parameter optimization test scheme*

The Box-Behnken design experimental design in Design Expert software was used to analyse a 3-factor, 3-level response surface test for the soil splitting angle α, forward tilt angle β, and forward speed of the unit v. In the test, the forward resistance Q (N) and the width of the low border W (mm) were used as the test indexes for the response (*Asaf et al., 2007; Mak et al., 2012; Shmulevich et al., 2010*), and Table 2 shows the coding of the established test factors.

Table 2

Factors and coding of the experiment

Numbers	Factors		
	Factor A: Partition angle α / (°)	Factor B: top rake β / (°)	Factor C: Unit forward speed *v* / (km·h^{-1})
-1	55	45	7
0	60	60	8
1	65	75	9

Based on the above test factor coding table, the design of the test protocol was carried out with a total of 17 sets of tests, of which 12 sets were used as analytical factorization points 5 sets were used as nulls, and the null tests were repeated several times to estimate the experimental error. The experimental protocol and results are shown in Table 3. The forward resistance variance and low-border width variance were also analysed based on the experiments *(Choudhary et al., 1985)*.

Table 3

Response surface analysis and test results

Numbers	Factor X1	Factor X2	Factor X3	Forward resistance T / (N)	Low border width W / (mm)
1	1	-1	0	1234.8	532.32
2	1	1	0	1181.1	526.78
3	0	0	0	981	533.16
4	1	0	-1	1082.8	534.8
5	0	0	0	981	533.16
6	0	-1	-1	990.4	536.92
7	0	1	1	1045.8	532.9
8	0	0	0	981	533.16
9	-1	0	1	1022.6	547.08
10	0	0	0	1021.3	529.3
11	-1	1	0	923.8	533.8
12	0	0	0	1021.3	529.3
13	-1	0	-1	1052.1	533.86
14	0	-1	1	1184	539.04
15	1	0	1	1254.1	529.08
16	-1	-1	0	1025	534.02
17	0	1	-1	924.5	540.18

By analysing the forward resistance ANOVA and low border width ANOVA. The results show that only the interaction of model X_1X_3 has a significant effect on forward resistance as well as low-border width, so the response surface analysis was performed. When the front inclination angle β is 60°, the relationship between the soil dividing angle and the forward speed of the unit and the forward resistance and the width of the low border is obtained as:

$$T = 16171.608 - 458.374X_1 - 545.313X_3 + 10.04X_1X_3 + 3.302X_1^2 \tag{4}$$

$$W = 441.91 + 6.932X_1 - 0.947X_1X_3 + 5.066X_3^2 \tag{5}$$

The specific rule of change is shown in Fig. 5(a). When the front inclination angle β is 60°, the forward resistance of the ridging device decreases with the forward speed of the unit, and the decrease in the soil dividing angle shows a decreasing and then slightly increasing trend. According to the plough's traction resistance rational formula, it can be seen that the smaller the forward speed of the unit, the forward resistance of the ridging device decreases. However, when the soil dividing angle is too small, the length of the ridging device will increase to satisfy the low-border width agronomical requirements. This leads to an increase in the force area in the forward direction of the unit, thus its forward resistance shows a slightly increasing trend. For the change of the width of the low border, the width of the low border needs to be maintained at about 54 cm. From Fig. 5(b), it can be seen that the width of the low border tends to decrease and then increase as the angle of parting decreases and the forward speed of the unit increases. The throwing distance of the soil particles in the forward direction of the unit is not enough to affect the bordering operation of the ridging device. Through the structure design of the ship-type ridging device, the low border's width is relatively increased, which meets the corresponding agronomic requirements.

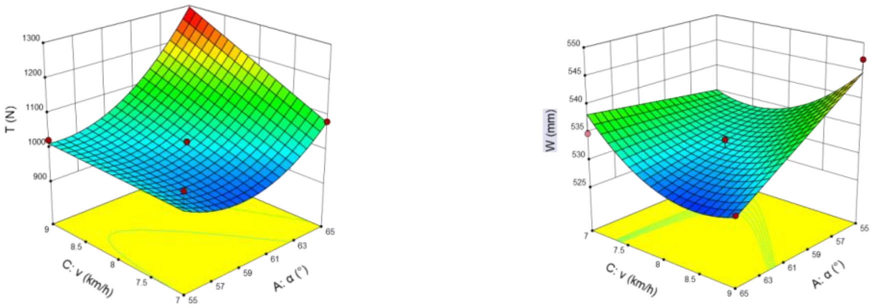

(a) (b)

Fig. 5 - The response surface of the soil dividing angle and the forward speed of the unit to the forward resistance and the low border width

From the above response surface analysis, it can be seen that the three factors of soil parting angle, forward tilt angle, and forward speed of the unit will have interactive effects on the forward resistance and the width of the low border, therefore, the regression model was solved by applying Design-Expert software to optimize the regression model under the objective to obtain the best combination of parameters, and the optimization constraints are:

$$\begin{cases} \min T \\ 538\text{mm} \leq W \leq 542\text{mm} \\ s.t.\begin{cases} 55° \leq \alpha \leq 65° \\ 45° \leq \beta \leq 75° \\ 7\text{km/h} \leq v \leq 9\text{km/h} \end{cases} \end{cases} \tag{6}$$

The optimal parameter combinations were calculated as follows: 61.46° dividing angle, 64.98° forward tilt angle, 7.01 km/h forward speed of the unit, 923.80 N forward resistance, and 538.08 mm width of the low borders, which were rounded off to take the dividing angle of 61°, the forward tilt angle of 65°, and the forward speed of the unit of 7 km/h.

Layout of ridging device and stubble removal device design

To reduce the number of implements in the ground, the ridging device is set to construct two raised borders, one low border, and two half-low borders at a time. Install a soil scraper in the middle of the centre border builder and in the middle of the side border builder to level the surface of the high borders. The specific structure of the ridging device is shown in Fig. 6 (a).

To prevent the throwing of soil to bury the completed sowing rows during the process of rotary tillage and stubble removal, the direction of the rotary ploughing curved knives is rearranged. The rotary ploughing curved knives in the low borders are bent in the direction of the high borders and the straight knives are used in the high borders, to mix the stubble with the soil sufficiently and not throw the soil particles out of the outside of the machine tool, which can reduce the energy consumption. The specific structure is shown in Fig. 6 (b).

(a) (b)

Fig. 6 - Ridging device layout diagram and structure drawing of rotating tillage stubble removal device

Field experiment

Test conditions

Test prototype in Shandong Qingyun Yiyuan Agricultural Machinery Manufacturing Co., Ltd. trial, the test site for the Zibo Aimin Seed Industry Yellow River Beach test base, the use of "Kaite Shenzhou red 1804" tractor as supporting power, Figure 7 for the field test photos.

Fig. 7 - Prototype field test diagram

Test methods and contents

According to the national standard GB/T 20865-2007 "No Tillage Fertilization Seeder", this article tested the testing indicators for the sowing quality of wheat no tillage seeders and the requirements for high and low borders wheat planting modes. The main equipment used includes electronic scales, tape measure, board ruler, small shovel, plastic bags, etc. The wheat variety used in the test was blue wheat developed by Aimin Seed Industry, and the sowing rate of 187.5 kg/hm^2 was set in the test; the fertilizer was compound fertilizer, and the fertilizer application rate was 675 kg/hm^2*(Liu et al., 2011)*. The sowing speed was 7km/h.

(1) ***Machine passability***

The tractor will pass if it operates at a predetermined speed and makes one round trip with the previous crop covered with straw without heavy blockage.

(2) ***Seeding depth and seedling strip width***

The tractor was operated at a predetermined speed, 3 rows of raised borders and 3 rows of low borders were randomly selected, and 5 points were taken from each row within a 100 cm area, the soil layer was peeled back to measure the depth of wheat seeding as well as the width of seedling belt, and the data were recorded.

(3) ***Height difference between high and low borders and width of borders***

The planter was operated at a predetermined speed, 3 rows of high borders and 3 rows of low borders were randomly selected, and the length of each row was randomly selected as a test area of 5 m. The width of the borders as well as the difference in height between the high and low borders were randomly measured in 5 places in the test area.

RESULTS

After the planter completed the operation, the seeding depth, seedling strip width, height difference between high and low borders, and border width were measured and recorded according to the test method, and the specific data are shown in Table 4.

Table 4

Test result

Detection area	Sowing depth /cm	Belt width /cm	High and low borders height difference / cm	Border width / cm
1	3.00	9.47	9.38	52.54
2	3.50	9.44	9.14	52.30
3	3.19	9.27	9.56	51.96
4	3.03	9.39	9.18	52.30
5	3.17	9.33	8.96	51.90
6	3.14	9.49	9.32	52.06
Average	3.17	9.40	9.26	52.18
Qualified rate /%	95.00	91.67	100.00	100.00
Standard deviation /cm	0.38	0.29	0.35	1.00
Variable coefficient /%	12.06	3.09	3.83	1.93

The experimental results show that the seeding depth qualification rate of this planter is high, but the double disk opener itself has the characteristic of soil return, resulting in the seeding depth of some positions of the seedling belt changing. The coefficient of variation is larger; the effect of soil return on the width of the seedling belt is also smaller, so the coefficient of variation is smaller. The height difference between the high and low borders and the width of the borders are high, and the coefficients of variation are small, which are in line with the relevant agronomic requirements and standards.

The specific seedling emergence situation is shown in Fig. 8, the wheat seedling emergence results are good and the height difference between high and low borders meets the test requirements. After harvesting wheat, the yield of the traditional border wheat planting pattern was 9732 kg/hm^2, and the yield of the high and low border wheat planting pattern was 10745 kg/hm^2, which was up to 10.4%, and the effect of yield increase was obvious. The irrigation area was smaller than that of traditional border cropping, and the water saving could be up to 40%.

Fig. 8 - The emergence of wheat

CONCLUSIONS

(1) Aiming at the problems of low land utilization and serious waste of water resources in the existing wheat planting pattern, a two-high and two-low wheat high-low border planting pattern was proposed, and a no-tillage sowing machine for high and low borders was designed, which integrates stubbing, fertilizer application, border construction, and seeding.

(2) A ship-type ridging device was designed, the main influencing factors affecting the border construction resistance and the width of the low border were determined. The simulation test was carried out on the border construction process, and the optimal parameters were obtained after data processing. When the dividing angle α of the trellis is 61°, the forward inclination angle β is 65°, and the forward speed v of the unit is 7 km/h, the resistance of the ridging device is minimized under the condition of satisfying the width of the low border. The rotating stubble device was designed so that based on the completion of the stubbing operation, it can concentrate the soil of the low-border border towards the high-border border to reduce the resistance of the border construction.

(3) A field test was conducted, and the test data were analysed. According to national standards, the planter made three round trips within the 60 m test operating area without any serious blockage, and the machine had good passability. The average value of the sowing depth of the no-tillage wheat planter in the high and low borders was 3.17 cm, the qualification rate was 95%, the standard deviation was 0.38 cm, and the coefficient of variation was 12.06%. The average value of the width of the seedling belt was 9.40 cm, the qualification rate was 91.67%, the standard deviation was 0.29 cm, and the coefficient of variation was 3.09%. The average height difference between the high and low borders was 9.26 cm, the pass rate was 100%, the standard deviation was 0.35 cm, and the coefficient of variation was 3.83%. The average width of the borders was 52.18 cm, the qualified rate of the border width was 100%, the standard deviation was 1.00 cm, and the coefficient of variation was 1.93%. Finally, the differences between each index and the theoretical design are small and meet the agronomic requirements.

REFERENCES

[1] Asaf Z, Rubinstein D, Shmulevich I., (2007). Determination of discrete element model parameters required for soil tillage [J] (Shmulevich I. Determination of discrete element model parameters required for soil tillage) *Elsevier BV*, no.1, pp.227-242.

[2] Chiming Qi., (2020). Analysis of domestic wheat market situation [J] (国内小麦市场形势分析). China's national conditions and national strength, no. 10, pp. 60-62;

[3] Choudhary M.A., Yu Guo-Pei, Baker C.J., (1985). Seed placement effects on seedling establishment in direct-drilled fields [J] (Seed placement effects on seedling establishment in direct-drilled fields). *Elsevier BV*, no.1, pp. 79-93;

[4] Deping Song, Wei Li, Mingjun Li et al., (2021). Design and experiment of wheat high-low-border wide-seedling belt planter [J] (小麦高低畦宽苗带播种机设计与试验). *Journal of Chinese Agricultural Mechanization*, vol.42, no.3, pp. 1-6;

[5] Han X.M., Wang H.Y., (2005). The Analysis and Dynamic Emulation of the Cam Mechanism Based on ADAMS/View [J] (基于 ADAMS/View 机心凸轮机构分析与动态仿真). *Mechanical Engineer*, no.10, pp. 97-99;

[6] Jiancang Yang., (2008). *Study on the Development of Wheat Production and the Support of Science and Technology in China* [D] (我国小麦生产发展及其科技支撑研究). Chinese Academy of Agricultural Sciences.

[7] Jinbao Liu, Qingchao Li, Xuan Zheng et al., (2012). Research Status of Drag Reduction Technology for Soil Tillage Components [J] (土壤耕作部件减阻技术研究现状). *Xinjiang Agricultural Mechanization*, vol.37, no.6, pp. 25-28;

[8] Kaituo Fang, Hailang Ge, Yunyang Shi et al., (2019). Optimization and simulation of profile spraying mechanism based on ADAMS [J] (基于 ADAMS 的果树仿形施药机构优化设计与仿真分析). *Journal of Chinese Agricultural Mechanization*. vol.40, no.10, pp. 58-63;

[9] Lite LI., (2006). The opportunity for the development of China's wheat industry lies in the modernization of traditional staple food (中国小麦产业发展的机遇在于传统主食现代化). *Grain Processing*, no.4, pp.5-8;

[10] Liu L., Liu Z., Yang X. et al., (2011). Design and test on pneumatic no-till wheat planter [J] (气流输送式小麦免耕播种机设计和试验). *Transactions of the Chinese Society for Agricultural Machinery*, vol.42, no.2, pp. 54-57;

[11] Mak J., Chen Y.,Sadek M.A., (2012). Determining parameters of a discrete element model for soil–tool interaction [J] (Determining parameters of a discrete element model for soil–tool interaction) *Elsevier BV*, pp. 117-122;

[12] Shan Gao., (2020). Present situation and development countermeasures of wheat industrialization in China [J] (中国小麦产业化现状与发展对策). *Agricultural development and equipment*, no.3, pp. 25-26;

[13] Shmulevich I., (2010). State of the art modeling of soil–tillage interaction using discrete element method [J] (State of the art modeling of soil–tillage interaction using discrete element method). *Elsevier BV,* no.1*,* pp. 41-53;

[14] Shuhong Zhao, Enchen Jiang, Yixun Yan, et al., (2013). Design and motion simulation of opener with bidirectional parallelogram linkage profiling mechanism on wheat seeder [J] (基于 ADAMS 的播种机仿形机构运动仿真). *Transactions of the Chinese Society of Agricultural Engineering*, vol.29, no.14, pp. 26-32;

[15] Songlie Yu., (1980). High-yield cultivation of winter wheat by fine sowing [J] (冬小麦精播高产栽培). Journal of Shandong Agricultural College, no.2, pp. no.3, pp. 25-26;

[16] Wen Gou, Rongchao Ma, Wenyu Yang et al., (2012). Design of opener on no-till wheat seeder. *Transactions of the Chinese Society of Agricultural Engineering* [J], vol.28, no.S1, pp. 21-25;

[17] Wenyan Yao, Dianbao Zhao, Guangfei Xu et al., (2020). Design and experiment of non-blocking device for no-tillage seeding of maize with active strip-to-row [J] (条带对行主动式玉米免耕播种防堵装置设计与试验). *Transactions of the Chinese Society for Agricultural Machinery*, vol.51, no.S2, pp. 55-62+71;

[18] Xiaopeng Liu, Wenli Xiao, Lei Ma et al., (2017). Design and Ditching Quality Experiment on Combined Ship TypeOpener of Direct Rapeseed Seeder [J] (油菜联合直播机组合式船型开沟器设计与开沟质量试验). *Transactions of the Chinese Society for Agricultural Machinery*, vol.48, no.11, pp. 79-87; (in Chinese with English abstract)

[19] Xiaopeng Liu, Qingsong Zhang, Lichao Liu, et al., (2019). Surface Optimization of Ship Type Ditching System Based on Differential Geometry and EDEM Simulation [J] (基于微分几何与 EDEM 的船型开畦沟装置触土曲面优化). *Transactions of the Chinese Society for Agricultural Machinery*, vol.50, no.8, pp. 59-69; (in Chinese with English abstract)

[20] Xiaobing Fan, (2016). Research on corn no-tillage planner and its key components in wheat stubble fields [D] (麦茬地玉米免耕播种机及其关键部件的研究). *Nanjing Agricultural University*.

[21] Zhen Ji, Zhigang Liu, Jiannan Yu, et al., (2021). Design and simulation analysis of copying mechanism of shrub stubble machine [J] (灌木平茬机仿形机构的设计及仿真分析). *Machinery Design and Manufacture*, no.8, pp. 70-74;

[22] Zhuang W.D., Wang C., Wang X., (2006). The Analysis and Operating Setup for Flexi-Coil's Variable Planter [J] (Flexi-Coil 变量播种机使用设置的分析). *Journal of Agricultural Mechanization Research*, vol.60, no.3, pp. 56-57.